

## Spectroscopic observations of the radiative charge transfer and association of helium ions with neon atoms at thermal energy

Rainer Johnsen

*Department of Physics and Astronomy, University of Pittsburgh, Pittsburgh, Pennsylvania 15260*

(Received 23 September 1982)

The radiation emitted by the radiative charge transfer  $\text{He}^+ + \text{Ne} \rightarrow \text{He} + \text{Ne}^+ + h\nu$  has been observed with the use of a selected-ion drift apparatus in conjunction with spectroscopic instrumentation. The two observed emission features with wavelengths around 4100 and 4240 Å evidently arise from transitions in the short-lived  $\text{HeNe}^+$  excited molecular ion which is formed in the collision. Mass-spectrometric observations of the product ions indicated that the reaction occurred with a rate coefficient of  $1 \pm 0.3 \times 10^{-15} \text{ cm}^3/\text{sec}$  at a gas temperature of 300 K. In addition to charge transfer, a second associative reaction channel producing  $\text{HeNe}^+$  ions is found to have an effective rate coefficient of about  $2 \times 10^{-16} \text{ cm}^3/\text{sec}$ .

### I. INTRODUCTION

A slow collision between an ion  $A^+$  and an atom  $B$  of lower ionization potential than that of  $A$  may be viewed as a transient formation of an excited state of the molecular ion  $AB^+$ . If during the short lifetime of this state a radiative transition to the energetically lower charge-exchanged state takes place, the overall result of the collision may be either radiative charge transfer (RCT)



or radiative association

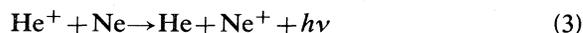


Both processes may occur in parallel with relative probabilities a function of the collision energy, the impact parameter, and the  $A^+-B$  and  $A-B^+$  interaction potentials. These radiative collision processes involve radiative transitions between molecular states and should be clearly distinguished from charge-transfer collisions which leave one of the colliding particles in an excited state which subsequently undergoes a radiative transition to a lower atomic state. The latter type of process, usually described by a "curve-crossing" mechanism, may occur with very high probability in cases where suitable final states are available. By contrast, radiative charge transfer and association are intrinsically very improbable, typically exhibiting cross sections on the order of  $10^{-5}$  or less of the elastic scattering cross section.

With the exception of perhaps some astrophysical environments, radiative charge transfer is not generally a determining factor in the ionization balance

of ionized media, and hence comparatively little effort has been spent on their theoretical or experimental study. There are cases, however, where RCT appeared to be the only possible charge-transfer mechanism, and in a series of recent measurements<sup>1</sup> this mechanism was invoked to explain the experimental findings, although the emitted radiation was not actually observed. The suggestions seemed well founded, at least in the case of the reaction  $\text{He}^{2+} + \text{He} \rightarrow \text{He}^+ + \text{He}^+ + h\nu$ , since an *ab initio* theoretical calculation<sup>2</sup> gave results in close agreement with the experimental cross section. It was therefore interesting to see if the radiation emitted by RCT could be observed in a laboratory experiment. A further motivation for this study arose from the close connection between radiative charge transfer and its inverse process, charge transfer induced by strong radiation fields, which is currently a topic of considerable experimental<sup>3</sup> and theoretical activity.

In multiple-collision experiments, such as used for this study, the smallness of the RCT cross section is not a serious hindrance, since it can largely be compensated for by increasing the ion-atom collision frequency, i.e., increasing the density of target atoms. The occurrence of charge transfer and association as a result of triple collisions introduces some interpretational difficulties, however, because the formation of bound, excited molecular ions can make a contribution to the observed spectra. The reaction of  $\text{He}^+$  ions with neon



was chosen primarily because the expected emission features fall into a favorable spectral range, but it

also proved to be a fortunate, although not ideal, system to study because the formation of bound, excited  $\text{HeNe}^+$  ions seems to be a minor effect in this case.

## II. EXPERIMENTAL TECHNIQUES AND APPARATUS

In principle, the experimental technique consisted of passing a mass-analyzed current of helium ions through neon gas and observing both the emitted radiation and the product ions by spectroscopic instrumentation and ion mass spectrometers, respectively. The apparatus used was the selected-ion drift apparatus (SIDA) shown schematically in Fig. 1. Except for the recent addition of the additional ion-selecting mass spectrometer between the ion source and the drift region, the apparatus has been used for a number of years for ion-molecule reaction studies and has been described in detail previously.<sup>4</sup>

For spectroscopic observations, a small volume of the drift region, located approximately in the middle of the drift tube, was imaged by a unit magnification lens and mirror system onto the entrance slit of a 0.3-m monochromator (McPherson model 218). The orientation was such that the monochromator's slit viewed an area perpendicular to the drift tube axis. The exit slit of the monochromator was imaged onto the photocathode of a photomultiplier tube (Hamamatsu type R585) which was thermoelectrically cooled to  $-5^\circ\text{C}$  in order to reduce dark counts, typically to 1.5 counts/sec. In the earlier stages of the experiment, a simpler optical system consisting of several narrow-band interference filters placed in front of a different phototube (EMI type 9558) was used. While this system had a better optical efficiency, it was later abandoned because of its limited coverage of the spectrum.

For time-resolved measurements, the ion source

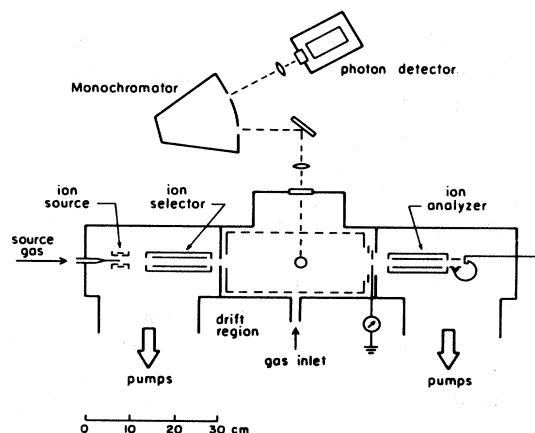


FIG. 1. Schematic diagram of the SIDA and the spectroscopic instrumentation used in this experiment.

was operated in a pulsed mode and both photon and ion counts were accumulated in a multiscaler over many experimental cycles. For recordings of the photon spectrum, the ion source was operated in a continuous mode. Photon counts were accumulated in a single-channel counter for periods of typically 60 sec, the number counted in that interval was then converted to an analog voltage and plotted as the  $y$  value on an  $x$ - $y$  chart recorder, whose  $x$  value was given by the wavelength of the scanning monochromator for that measurement.

The total ion current traversing the drift region (the length is 35.66 cm), in this case carried almost exclusively by helium ions, was measured by two electrometers connected to two exit electrodes of the drift region. One electrode, which also contained the small (0.05 cm in diam) exit orifice leading to the analyzing mass spectrometer, collected all ions with displacements less than 0.5 cm from the drift tube axis. The larger fraction of the ion current (usually  $>90\%$  of the total) was collected by the second, annular electrode, which accepted all ions with displacements between 0.5 and 1.9 cm from the drift tube axis. Less than 1% of all ions were found to have displacements larger than 1.9 cm; thus this part of the ion current was ignored. In order to obtain an adequate photon signal, it was necessary to inject  $\text{He}^+$  ion currents of about  $10^{-8}$  A into the drift tube, a value considerably larger than normally used in charge-transfer reaction-rate determinations. Smaller ion currents were employed in the measurements of product-ion arrival spectra in order to avoid possible space-charge effects in the drift tube.

All vacuum- and gas-handling systems were of ultrahigh vacuum quality, and the system was pumped to pressures below  $10^{-8}$  Torr between experiments. All gases used were of ultrahigh purity (supplied by Matheson Company); the role of residual impurities is discussed briefly in Sec. III D.

## III. MEASUREMENTS AND RESULTS

### A. Origin of the observed radiation

When a photomultiplier tube without any wavelength-selecting element was used to detect photons, a fairly strong photon signal (several hundred counts per sec) was observed, but the origin of this radiation was not clear. By operating the drift tube in the pulsed mode, it was established that photons were observable only when the  $\text{He}^+$  cloud was located under the observation window, thus ruling out photons produced in the ion source and a variety of other possible origins. By placing a 4100-Å interference filter (bandwidth  $\sim 100$  Å) in front of the phototube, it was found that the dominant fraction of the observed photons had wavelengths within the

bandwidths of this filter. Since the difference in ionization potentials of He and Ne corresponds to a wavelength of 4100 Å, this observation strongly suggested the  $\text{He}^+ + \text{Ne}$  charge transfer as the source of the radiation.

In a further test, the drift tube was filled with helium rather than neon. No radiation was detected with the 4100 Å filter in place, but some was found in spectrally unresolved light. The origin of this radiation was eventually traced to a reaction of  $\text{He}_2^+$  ions (formed by three-body association in helium gas) with a nitrogen impurity. The reaction of  $\text{He}_2^+$  with  $\text{N}_2$  is known to produce  $\text{N}_2^+(B)$  which decays by emission of the first negative band system of  $\text{N}_2^+$ . The strongest band at 3914 Å was detectable when a 3914-Å filter was used, and the intensity of this emission feature was found to increase when  $\text{N}_2$  was added to the helium. In neon gas  $\text{He}_2^+$  ions cannot form, and hence this source of radiation will not be present.

Excitation of neon atoms by energetic electrons had to be considered as a possible interfering effect, since electrons were known to be released by helium ions striking the exit electrodes of the drift region. In order to investigate this possibility, the drift tube was operated in the pulsed mode, and the drift field was turned off at the precise time when the  $\text{He}^+$  ion cloud was located under the observation window. The radiation persisted for the duration of the field interruption. Since, in the absence of the electric field, electrons would not attain sufficient energy to excite Ne atoms, the observed radiation was shown not to result from electron impact excitation.

The measurements employing filters were useful for initial tests but were later abandoned because of their poor spectral resolution and incomplete coverage of the spectrum. The measurements using a grating monochromator are described in the next section.

### B. Measured spectra

While the use of the grating monochromator to disperse the radiation entailed a considerable decrease in sensitivity, it proved feasible to scan the wavelength range from 3950 to 4300 Å with a resolution of 12 Å (full width of a triangular slit function at half maximum). Under the best conditions, neon pressures  $\sim 1.7$  Torr,  $\text{He}^+$  ion current  $\sim 10^{-8}$  A, and  $E/N = 6 \times 10^{-17}$  V cm<sup>2</sup>; the photon count rate at 4100 Å was typically 8 counts/sec. An example of a recorded spectrum is shown in Fig. 2. Before and after each spectrum was taken, parts of the spectral range were scanned under conditions where no helium ions were injected into the drift tube, but the ion source filaments, gas flow, etc., were left unchanged. The background count rate,

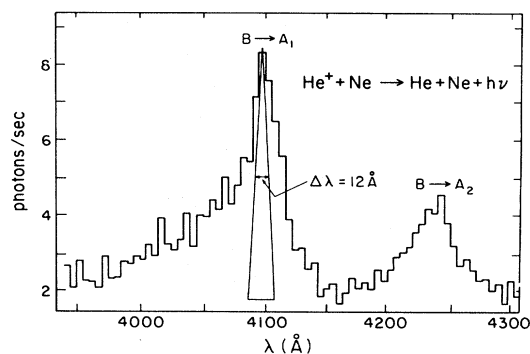


FIG. 2. Example of a spectrum observed at a helium pressure  $p(\text{He}) = 1.7$  Torr,  $E/N = 6$  Td, and a helium ion current of  $1 \times 10^{-8}$  A. The triangle shown at 4100 Å indicates the slit function of the monochromator.

including spurious photons from the ion source, was found to be independent of wavelength and was typically 1.5 to 2.0 counts/sec.

Similar spectra to those shown in Fig. 2 were taken for a variety of conditions; neon pressures between 0.6 and 2 Torr,  $E/N$  ranging from 5 to  $15 \times 10^{-17}$  V cm<sup>2</sup>, and different ion currents. Although the total intensity varied considerably with conditions, no significant variation of the spectral distribution of the radiation was found. As will be discussed later, the two distinct emission features resulting from transitions from a common upper state to two different lower states would not be expected to change their relative intensities with experimental conditions. This was found to be true; consequently, the subsequent measurements of the absolute intensities of the radiation with varying experimental conditions were carried out only on the more intense feature near 4100 Å.

### C. Variation of the intensity of the spectra with $\text{He}^+$ ion current, neon density, and $E/N$

A series of measurements was performed in which the intensity of the spectra was recorded at a fixed wavelength (4100 Å). As expected, the photon count rate at 4100 Å increased linearly as the injected  $\text{He}^+$  ion current was increased from  $10^{-9}$  to  $10^{-8}$  A. While deviations from a linear dependence might result from a spatial broadening of the  $\text{He}^+$  ion current at the higher currents, no such effects were large enough to be observed.

When the total ion current and the value of  $E/N$  were held constant, it was found that the intensity at 4100 Å also increased linearly with the neon pressure over the range 0.6–2.0 Torr. These measurements were intended to show that the photons were produced in a binary-collision process rather than by three-body collisions. None of the data points devi-

ated by more than 10% from a least-squares straight-line fit to the data; a quadratic dependence of the photon count rate on neon pressure, appropriate for a pure three-body process, would have led to a tenfold increase in intensity over the range of neon pressures investigated. A more detailed discussion of this experimental result will be given in Sec. IV.

In a further set of measurements, the neon pressure and the  $\text{He}^+$  ion current were held constant and the intensity at 4100 Å was recorded as a function of the  $\text{He}^+$  ions drift velocity  $v_d$ . Since for a constant ion current the ion density varies as  $1/v_d$ , the photon production rate is expected to show a similar  $1/v_d$  dependence as long as the reaction producing the photons does not itself also vary with the ion velocity or energy. The experimental observations, carried out between  $E/N$  values of  $3 \times 10^{-17}$  and  $11 \times 10^{-17}$  V cm<sup>2</sup>, supported this simple expectation, but a slight, about 20%, excess of photon counts was seen at the highest  $E/N$ . The range of ion energies covered by these experiments was small; at the highest  $E/N$  the  $\text{He}^+$  ions possess only about twice thermal energy. The measurements indicate, however, that the reaction producing the photons is not likely to exhibit a strong dependence on energy. An extension of the energy range was not practical because of the weak photon signal at high  $E/N$ .

#### D. Observations of product ions

Observations of product ions were carried out with the ion source operating in the pulsed mode, i.e., helium ions were injected into the drift region in the form of short pulses, typically 10-μsec long, repeated every few milliseconds. This mode of operation offered the advantage over measurements of the overall intensities of the product ions that additional information could be derived from the observed structure of the product-ion arrival time spectra. The large difference between the ionic mobilities of  $\text{He}^+$  and  $\text{Ne}^+$  ions in neon ( $\mu_0 = 18.4$  cm<sup>2</sup>/V sec for  $\text{He}^+$ , compared to  $\mu_0 = 4.1$  cm<sup>2</sup>/V sec for  $\text{Ne}^+$ ) provides rather favorable conditions for the analysis of the product-ion arrival spectra.

Ideally, only helium ions and the products of the reaction of  $\text{He}^+$  ions with neon should be present in the drift tube, but some minor deviations from this ideal behavior were observed. Some  $\text{Ne}^+$  ions, for instance, were found to be produced near the drift-tube entrance orifice when  $\text{He}^+$  ions were injected at energies in excess of 20 eV. These neon ions were clearly not the result of the RCT under study but were produced by a fast charge transfer with a threshold near 20 eV. By reducing the injection energy to about 15 eV, this effect could be eliminated. There was also evidence that some  $\text{He}^+$  ions were

produced in high-lying metastable states. Collisions of these metastable  $\text{He}^+$  ions with neon apparently were responsible for a very small signal of  $\text{Ne}^{2+}$  ions that was generally present in the experiments.

A further minor perturbation was found to result from the electrons released from the drift-tube exit electrodes by impinging  $\text{He}^+$  ions. Under conditions of low pressure and high  $E/N$ , these were capable of ionizing neon atoms in the drift space, leading to several small peaks superimposed on the  $\text{Ne}^+$  arrival time spectra. (The sensitivity of these peaks to magnetic fields applied near the drift tube exit indicated that charged particles rather than uv photons were responsible.)

Several impurity ions were observed, of which only  $\text{N}^+$  and  $\text{N}_2^+$  seemed strong enough to warrant concern. Estimates based on the known rate coefficient for the charge-transfer reaction  $\text{He}^+ + \text{N}_2$  and the observed count rates of  $\text{N}^+$  and  $\text{N}_2^+$  indicated a presence of about 0.3 ppm of  $\text{N}_2$  in the neon gas. Since the concentration of  $\text{N}_2$  could not be reduced further, the sensitivity of the  $\text{Ne}^+$  arrival time spectra to measured additions of  $\text{N}_2$  was also investigated. A tenfold increase of the  $\text{N}_2$  concentration was required to produce a measurable effect on the  $\text{Ne}^+$  signal. With only the normal impurity concentration present, the effect of  $\text{N}_2$  should have been completely negligible.

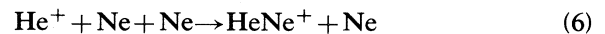
As expected,  $\text{Ne}^+$  ions were found to be the dominant product of the reaction of  $\text{He}^+$  ions with neon, but a smaller, secondary product ion  $\text{Ne}_2^+$  was also observed. An analysis of the structure of the  $\text{Ne}_2^+$  arrival spectra showed that only part of the  $\text{Ne}_2^+$  ions was produced by the reaction



followed by three-body conversion



A second mechanism, consisting of three-body association



or radiative association



followed by the fast secondary reaction ( $k = 1.4 \times 10^{-10}$  cm<sup>3</sup>/sec (Ref. 5))



was required to reproduce the observed  $\text{Ne}_2^+$  arrival spectra, as shown below.

With the help of Fig. 3 it is not difficult to see how the product-ion arrival spectra are produced. In Fig. 3(a) the path of a pulse of helium ions

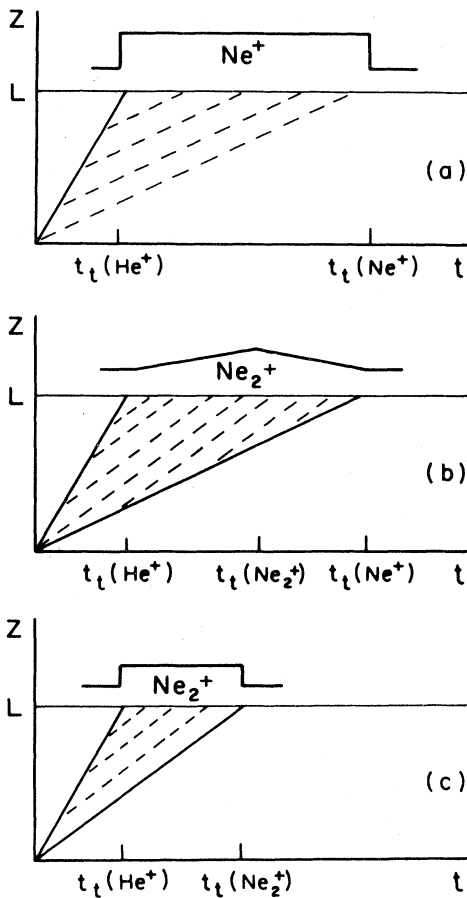


FIG. 3.  $z, t$  diagrams of the paths of the parent ions and their reaction products through the drift tube. (a) Production of  $Ne^+$  from the  $He^+ + Ne$  reaction. (b) Production of a secondary arrival spectrum of  $Ne_2^+$  ions from three-body conversion of  $Ne^+$  ions. (c) Production of a secondary  $Ne_2^+$  arrival spectrum via reactions (6) and (7) followed by fast conversion to  $Ne_2^+$  in reaction (8).

through the drift tube is shown in the form of a  $z, t$  diagram, where  $z$  denotes the distance in the drift direction, measured from the entrance of the drift tube, and  $t$  denotes the time, measured from the time of injection. In order to keep the figures simple, the effect of diffusive spreading of the helium ion pulse and the slight reactive loss of  $He^+$  ions (several percent in one transit time) have been ignored. The probability of producing a neon ion is thus constant along the path of the helium ion pulse, and a constant number of  $Ne^+$  ions will arrive at the collector end of the tube between the transit times of  $He^+$  ions. The expected shape of the  $Ne^+$  arrival spectrum closely matches that observed in the experiment (see Fig. 4).

The small fraction of  $Ne^+$  ions undergoing three-body conversion to  $Ne_2^+$  ions give rise to a second-

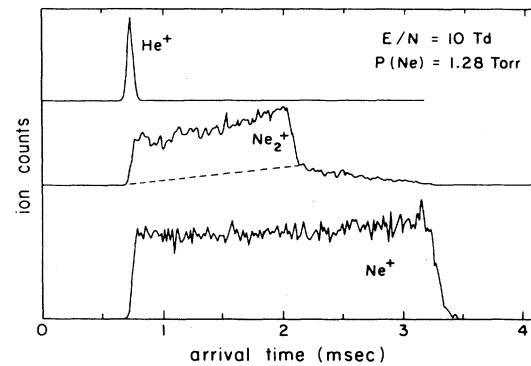


FIG. 4. Example of arrival spectra of the parent ion  $He^+$  and the secondary and primary product ions  $Ne_2^+$  and  $Ne^+$ . Dashed line drawn in the  $Ne_2^+$  arrival spectrum indicates the decomposition into the two parts discussed in the text.

dary arrival spectrum of  $Ne_2^+$  of a triangular shape, such as shown in Fig. 3(b). The shape results from the fact that the density of  $Ne^+$  ions, the parent ion of  $Ne_2^+$ , is approximately constant within the area bounded by the line  $z=L$  and the two rays from the origin to the points where  $z=L$  and  $t=t_1(He^+)$  or  $t=t_2(He^+)$ . The intensity of  $Ne_2^+$  ions arriving at times between  $t_1(He^+)$  and  $t_2(He^+)$  in this case is proportional to the integrated density of  $Ne^+$  ions along lines parallel to  $z=v(Ne_2^+)t$ . A triangular shape with the apex at  $t=t_2(He^+)$  results, but a comparison with the experimental  $Ne_2^+$  arrival spectrum (Fig. 4) shows that an additional contribution  $t_1(He^+)$  and  $t_2(Ne_2^+)$  is present from a different source.

Reactions (6) and (7) followed by rapid conversion of  $HeNe^+$  ions to  $Ne_2^+$  can provide this additional contribution. The time required for the secondary reaction in this case is negligible and a simple, rectangular arrival spectrum between  $t_1(He^+)$  and  $t_2(Ne_2^+)$  should be observed [see Fig. 3(c)]. A superposition of both the triangular and the rectangular shapes reproduces the experimental arrival spectra (Fig. 4) quite well.

The qualitative analysis of the arrival spectra serves mainly to identify the origin of observed product ions. In principle, rate coefficients can be derived from the observed shapes of the arrival spectra, but in the case of very slow reactions this method gives rather inaccurate results. Under typical conditions, the depletion of  $He^+$  ions in one transit time amounts to only a few percent, and it would be difficult to infer the exact loss rate from the observed product-ion arrival spectra. Thus an alternate method was used in which the absolute number of product ions produced in a given time was measured in order to obtain rate coefficients.

### E. Absolute intensities of parent and product ions

Under typical conditions [ $p(\text{Ne}) \approx 1$  Torr,  $E/N \approx 10$  Td, and  $t_t(\text{He}^+) \approx 500$   $\mu\text{sec}$ ] the count rates of both product ions  $\text{Ne}^+$  and  $\text{Ne}_2^+$  were only small fractions (0.5–3 %) of the  $\text{He}^+$  count rate, indicating a very slow conversion of  $\text{He}^+$  ions.

The rate coefficients were obtained by measuring the  $\text{He}^+$  ion count rates  $n(\text{He}^+)$  and those of the product ions under identical conditions. From the observed ratios of count rates, the rate coefficient was then obtained from the relationships

$$n(\text{Ne}^+)/n(\text{He}^+) = k_1[\text{Ne}]t_t(\text{He}^+) \quad (9)$$

and

$$n(\text{Ne}_2^+)/n(\text{He}^+) = k_2[\text{Ne}]t_t(\text{He}^+), \quad (10)$$

where  $k_1$  is the rate coefficient for reaction (4) and  $k_2$  is the combined rate coefficient for reactions (6) and (7).  $[\text{Ne}]$  is the concentration of neon and  $t_t(\text{He}^+)$  the measured transit time across the drift region of  $\text{He}^+$  ions. The numbers  $n(\text{Ne}^+)$  and  $n(\text{Ne}_2^+)$  were taken from the arrival spectra of those ions, subtracting in the case of  $\text{Ne}_2^+$  that part arising from three-body conversion of  $\text{Ne}^+$  ions.

Since this method of analysis assumes equal sensitivities for detecting different ions, tests were made by injecting  $\text{Ne}^+$  ions into the drift region and relating the measured count rate from the mass spectrometer to the observed  $\text{Ne}^+$  ion currents to the exit orifice, measured by an electrometer. The ratios were quite similar to those found in the case of  $\text{He}^+$  ions, indicating nearly equal sensitivities for both ions. In practice, it was found difficult to obtain reproducible transmission through the quadrupole mass spectrometer, and day-to-day variations of 20–30 % were quite common. These measurements of count rates yielded the values  $k_1 = (1 \pm 0.2) \times 10^{-15}$  and  $k_2 = (0.2 \pm 0.05) \times 10^{-16}$   $\text{cm}^3/\text{sec}$ . Previous measurements,<sup>1</sup> in which the rate coefficient was derived from the measured loss of  $\text{He}^+$  ions in neon, gave the value  $k_t = (k_1 + k_2) = (1 \pm 0.5) \times 10^{-15}$   $\text{cm}^3/\text{sec}$ , which is quite compatible with the present result obtained from the product-ion intensity determinations.

Considerable effort was spent on studying the pressure dependence of  $k_1$  and  $k_2$ . A series of measurements was made in which the ratio  $k_2/k_1$  was determined at different neon pressures (between 0.5 and 2 Torr), since it was thought that the relative contributions of the associative reactions (6) and (7) could be determined in this manner. No systematic variation of  $k_1$  was found over the range of neon pressures accessible (0.5 to 2 Torr), but the ratio  $k_2/k_1$  increased slightly with increasing neon pressure. A discussion of this result is given in Sec. IV.

### F. Measurements at 77 K

In order to elucidate the possible role of three-body reactions in these measurements, determinations of the  $\text{He}^+$  conversion-rate coefficient and the product-ion arrival spectra were also carried out at a reduced temperature of 77 K. The small apparatus<sup>6</sup> used in these studies was considerably simpler than that employed for the 300-K measurements, not having a mass-selective ion source and not being suitable for spectroscopic observations. However, it was possible to determine the rate coefficient for helium ions reacting with neon atoms and to obtain branching ratios for the production of bound  $\text{HeNe}^+$  and  $\text{Ne}^+$  ions. From the loss rate of  $\text{He}^+$  ions in neon, as determined by the additional residence time technique,<sup>4</sup> it was concluded that, at 77 K, the rate coefficient increased from a value of  $6.4 \times 10^{-15}$   $\text{cm}^3/\text{sec}$  to  $1.1 \times 10^{-14}$   $\text{cm}^3/\text{sec}$  when the neon density was increased from  $4.3 \times 10^{-16}$   $\text{cm}^{-3}$  to  $1.05 \times 10^{-17}$   $\text{cm}^{-3}$ , indicating that at this temperature the reaction contains a three-body contribution. By contrast to the measurements at 300 K, the dominant product ion was  $\text{HeNe}^+$ , as inferred from the secondary product ion  $\text{Ne}_2^+$  produced by reaction (8) as described in Sec. III D. The ratio of  $\text{Ne}_2^+/\text{Ne}^+$  was typically on the order of 2.7 to 3.3, i.e., on the order of 75% of reactive collisions produced the bound state of the  $\text{HeNe}^+$  molecular ion.

## IV. DISCUSSION

The experimental data showed clearly that the observed radiation originated from reactive collisions of  $\text{He}^+$  ions with neon atoms, but the electronic transitions involved and the mechanism populating the radiating state remain to be identified. The second of the two tasks is the more difficult one, and much of this section is devoted to a discussion of the possible role of three-body collisions and their effect on the data.

Figure 5 shows a potential-energy diagram of the  $\text{HeNe}^+$  molecule obtained by Siska<sup>7</sup> by the Rydberg-Klein-Rees (RKR) fitting of the spectroscopic data by Dabrowski and Herzberg.<sup>8</sup> An additional state  $A^2\Pi_{3/2}$  has been calculated by Blint,<sup>9</sup> but it has been omitted from the diagram since, according to Dabrowski and Herzberg, radiative transitions from the  $B$  state to this state do not take place with measurable intensity. In RCT the  $B$  state of  $\text{HeNe}^+$  is formed in a collision of a  $\text{He}^+$  ion with a neon atom; subsequent to radiation into either the  $A_1$  or  $A_2$  state, the charge-exchanged particles separate, completing the charge transfer. As indi-

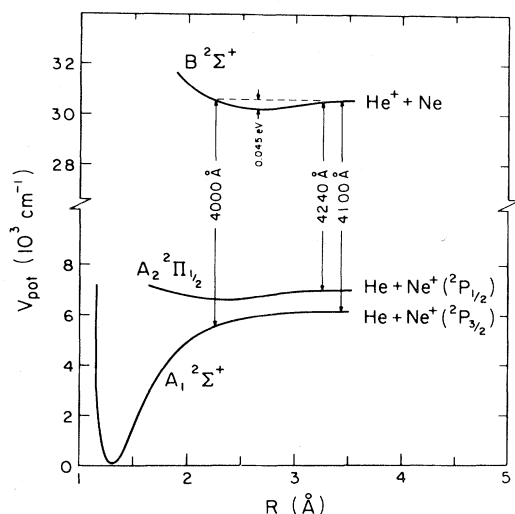


FIG. 5. Potential-energy diagram of the low-lying states of the  $\text{HeNe}^+$  ion, drawn after Siska's RKR fitting of the spectroscopic data by Dabrowski and Herzberg.

cated in the diagram, the  $B \rightarrow A_1$  transition energy corresponds to wavelengths between 4000 and 4100 Å depending on the internuclear separation at which the transitions take place. For  $B \rightarrow A_2$  transitions a narrow range of wavelengths around 4240 Å is emitted. These wavelengths agree with those of two observed emission bands leaving no doubt that the transitions have been correctly identified.

A quantitative analysis of the intensity distribution within the emission bands is beyond the scope of this investigation, but the spectra seem to bear out the qualitative expectation that the intensity maxima should occur at wavelengths corresponding to transitions at large internuclear separations. Close collisions, in which the particles approach distances below the repulsive radius of 2.2 Å should be very rare at thermal energies. The low intensity of the spectrum below 4000 Å in the  $B \rightarrow A_1$  band thus seems plausible. One would also expect that, with the possible exception of infrequent, nearly central collisions, most collisions would leave the charge-exchanges particles with sufficient kinetic energy to escape from the  $A_1$  potential well. The experimental finding that charge transfer dominated strongly over association at 300 K is in agreement with this expectation

This interpretation of the spectra as arising from binary  $\text{He}^+$ -Ne collisions is appealingly simple and

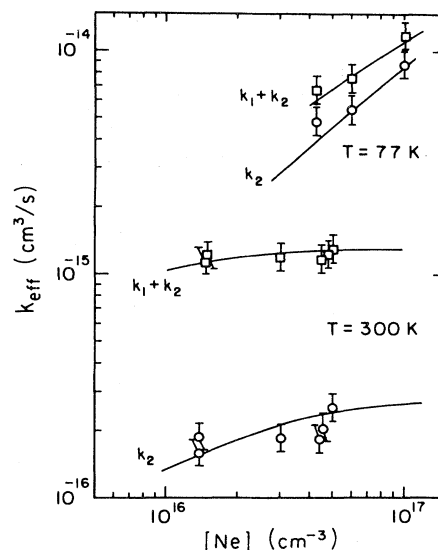
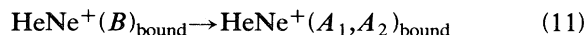
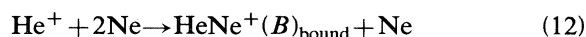


FIG. 6. Dependence of the observed rate coefficients on neon density and gas temperature. Lines drawn through the data points present a fit of Eq. (5) to the data with the parameters listed in Table I.

appears to be in harmony with experimental observations. One important consequence of this model could not be tested, however: The spectra should be essentially continuous with only a minor discrete component arising from inverse rotational predissociation. The experimental spectral resolution was insufficient to resolve a possible molecular-band structure in the spectra. Such structure could be present as a result of bound-bound transitions



in which the upper bound state is formed by three-body collisions



and is destroyed by both radiative transitions and collisional dissociation



A simple analysis of the corresponding three rate equations shows that the conversion frequency of  $\text{He}^+$  ions via this three-body path is given by

$$k^* = d\ln[\text{He}^+]/dt$$

TABLE I. Plausible parameters for the effective rate coefficient for conversion of  $\text{He}^+$  ions in neon.

$T$ (K)	$k^+$ ( $\text{cm}^6/\text{sec}$ )	$k^-$ ( $\text{cm}^3/\text{sec}$ )	$\nu_{\text{rad}}$ ( $\text{sec}^{-1}$ )	$k_{\text{rad}}$ ( $\text{cm}^3/\text{sec}$ )
300	$2.4 \times 10^{-32}$	$2 \times 10^{-10}$	$2.5 \times 10^6$	$1 \times 10^{-15}$
77	$1 \times 10^{-31}$	$3.6 \times 10^{-12}$	$2.5 \times 10^6$	$\sim 2 \times 10^{-15}$

$$= \nu_{\text{rad}} k^+ / k^- (1 + \nu_{\text{rad}} / k^- [\text{Ne}]), \quad (14)$$

where  $\nu_{\text{rad}}$  denotes the radiative decay frequency of Eq. (11), and  $k^+$  and  $k^-$  denote those rate coefficients of the inverse processes (12) and (13). Adding a rate coefficient  $k_{\text{rad}}$  for the purely binary reaction to this expression, the total effective rate coefficient for conversion of  $\text{He}^+$  ions in neon becomes

$$k_{\text{eff}} = k_{\text{rad}} + \nu_{\text{rad}} k^+ / k^- (1 + \nu_{\text{rad}} / k^- [\text{Ne}]). \quad (15)$$

Provided that  $k^- [\text{Ne}] \gg \nu_{\text{rad}}$  the second term in  $k_{\text{eff}}$  becomes independent of the neon density and the reaction will appear to have binary kinetics even though it contains a three-body contribution. Hence a sizable three-body contribution might exist in spite of the apparently binary reaction kinetics found experimentally (see Secs. III C and III E). No perfectly satisfactory method has been found to separate the relative contributions to  $k_{\text{eff}}$  in Eq. (15). The extreme assumption  $k_{\text{rad}} = 0$ , i.e.,  $\text{He}^+$  ions react by the three-body path only, can be ruled out though. The three-body coefficient  $k^+$  would have to have the unrealistically large value of  $3 \times 10^{-31} \text{ cm}^6/\text{sec}$  to obtain a value of  $k_{\text{eff}} = 10^{-15} \text{ cm}^3/\text{sec}$  independent of pressure with a 15% variation over the experimental range of neon pressures. Typical three-body association coefficients for rare-gas ions in rare gases are on the order of  $1 \times 10^{-31} \text{ cm}^6/\text{sec}$  (Ref. 10), and one would expect smaller rather than larger values for formation of the weakly bound  $\text{HeNe}^+(B)$  ion. Also, since the three-body reaction would result in bound  $\text{HeNe}^+$  ions it would be difficult to explain the dominance of charge transfer over association inferred from the observed product ions.

An attempt was made to choose plausible but not necessarily unique parameters for Eq. (15) such that the experimental data could be reproduced at both temperatures of 300 and 77 K. For the parameters listed in Table I,  $k_{\text{eff}}$  varies with  $[\text{Ne}]$  as shown in Fig. 6. The parameters were constrained by the condition that  $k^+ / k^-$  be on the order of  $10^{-22} \text{ cm}^3$  at 300 K, estimated from the theoretical expression for equilibrium constants of weakly bound van der Waals molecules given by Leckenby and Robbins.<sup>11</sup> An experimental value<sup>12</sup> for the clustering of  $\text{Li}^+$  ions in helium of  $k^+ / k^- = 1 \times 10^{-22} \text{ cm}^3$  may be adduced also since the ion  $\text{LiHe}^+$  has a binding energy of about 50 meV, close to that of  $\text{HeNe}^+(B)$ .  $k^-$  was assumed to vary with temperature in the form

$$k^- = k_L \exp(-D/kT),$$

where  $k_L$  is the Langevin rate coefficient for reaction (13). The radiative decay frequency  $\nu_{\text{rad}}$  of the

$B$  state was chosen such that  $k^* = k_2$ , i.e., the reaction channel leading to  $\text{HeNe}^+$  product ions is entirely ascribed to the three-body reaction. This assumption ignores a possible contribution from purely radiative association, reaction (7).

As may be seen in Fig. 6, the three-body contribution at 300 K is only about 20% of the total  $k_{\text{eff}}$  but is much larger at the reduced temperature of 77 K.  $k_{\text{eff}}$  is nearly independent of  $[\text{Ne}]$  at 300 K but increases with  $[\text{Ne}]$  at 77 K, in agreement with the measured rate coefficients. As stated earlier, the parameters in Table I cannot be uniquely determined from the data, but they do lead to a consistent description of the data at both temperatures.

In conclusion: Three-body effects are probably dominant at low temperatures, but they probably contribute only about 20% to the reaction at room temperature. The spectra at room temperature would therefore be expected to show a  $\sim 20\%$  contribution from bound-bound transitions. It may be of interest to note that the discharge spectra observed by Tanaka *et al.*<sup>13</sup> in rare-gas mixtures (including helium-neon) exhibited both a continuous and a discrete component and that the spectra could be enhanced by reducing the gas temperature. These observations may be related to the effects encountered here. It is possible that the reactions discussed in this article also provide the mechanism for excitations of the "helium-neon bands" which have been observed in electrical discharges (see Dabrowski and Herzberg<sup>8</sup> for a review and references to earlier work). It should be kept in mind, though, that a variety of other excitation mechanisms may exist in discharges which would be absent under the restricted conditions in drift-tube experiments.

## V. SUMMARY

The primary goal of this investigation has been to provide experimental evidence for our earlier suggestion that the  $\text{He}^+ + \text{Ne}$  charge transfer at thermal energies occurs in the form of radiative charge transfer. This objective has been achieved, and spectra of the emitted photons have been presented. It has also become apparent, though, that some complications arise in gas-phase measurements of this type from three-body collisions. In principle, the problems could be overcome by recording spectra with higher spectral resolution, which may be feasible with more specialized apparatus and better spectroscopic instrumentation.

## ACKNOWLEDGMENT

This research has been supported, in part, by the U. S. Army Research Office under Grant No. DAAG-29-80-K-0081.

- <sup>1</sup>R. Johnsen and M. A. Biondi, *Phys. Rev. A* **18**, 996 (1978).
- <sup>2</sup>J. S. Cohen and J. N. Bardsley, *Phys. Rev. A* **18**, 1004 (1978).
- <sup>3</sup>W. R. Green, M. D. Wright, J. F. Young, S. E. Harris, *Phys. Rev. Lett.* **43**, 120 (1979).
- <sup>4</sup>R. Johnsen and M. A. Biondi, *J. Chem. Phys.* **59**, 3504 (1973).
- <sup>5</sup>D. K. Bohme, N. G. Adams, M. Moseman, D. R. Dunkin, and E. E. Ferguson, *J. Chem. Phys.* **52**, 5094 (1970).
- <sup>6</sup>R. Johnsen, A. Chen, and M. A. Biondi, *J. Chem. Phys.* **72**, 3085 (1979).
- <sup>7</sup>P. E. Siska, *J. Chem. Phys.* **71**, 3942 (1979); and private communication.
- <sup>8</sup>I. Dabrowski and G. Herzberg, *J. Mol. Spectrosc.* **73**, 183 (1978).
- <sup>9</sup>R. J. Blint, *Phys. Rev. A* **14**, 971 (1976).
- <sup>10</sup>R. Johnsen, A. Chen, and M. A. Biondi, *J. Chem. Phys.* **73**, 1717 (1980).
- <sup>11</sup>R. E. Leckenby and E. J. Robbins, *Proc. R. Soc. London* **291A**, 389 (1965).
- <sup>12</sup>G. E. Keller and F. E. Niles, *Chem. Phys. Lett.* **10**, 526 (1971).
- <sup>13</sup>Y. Tanaka, K. Yoshino, and D. E. Freeman, *J. Chem. Phys.* **62**, 4484 (1975).